IET Research Journals

IET Journals
The Institution of Engineering and Technology

Testing of a hydro power plant's stability and performance using PMU and control system data in closed loop

ISSN 1751-8644
doi: 0000000000
www.ietdl.org

Sigurd Hofsmo Jakobsen, and Kjetil Uhlen

Department of Electric Power Engineering
Norwegian University of Science and Technology,
*Trondheim, Norway * E-mail: sigurd.h.jakobsen@ntnu.no*

Abstract: In response to recent concerns regarding deteriorating frequency quality in the Nordic power system, the Nordic transmission system operators (TSOs) have developed draft requirements for the provision of frequency containment reserves (FCR). These requirements outline extensive tests, which the power plant owners must perform to qualify to deliver FCR. In this paper we demonstrate that one can check these requirements by standard system identification techniques while the plant is in normal operation and by using measurements readily available from the plants control system or from a phasor measurement unit (PMU). The validity of the proposed method is demonstrated using Monte Carlo Simulation (MCS), where we investigate the effects of the main assumption and potential nonlinearities affecting the approach. Data from real power system operation is used to demonstrate the performance of the method.

1 Introduction

The Nordic TSOs have developed draft requirements for the frequency containment reserves (FCR)[6]. These requirements outline extensive tests, which the power plant owners have to perform to qualify to deliver FCR. In the proposed tests the power plant owners have to measure the plant's response to sine modulations of the input to the governor, while the plant is operating in open loop. These tests are then used for estimating the dynamics of the FCR. Since linear methods are used the procedure will have to be repeated for several operating states. A method similar to what is proposed in [6] is performed in [17], where system identification techniques are used on data from open loop sine tests to estimate models of hydro power plants.

The drawback with sine tests are that they are time consuming and expensive. Other approaches should therefore be investigated. In the literature it has been proposed to identify hydro power plant dynamics using data obtained from phasor measurement units (PMUs) during disturbances [1, 7, 15] and during normal operation [4, 8, 9, 11, 14]. Consequently, a natural next step is to investigate whether or not it can be checked if the plants are fulfilling the requirements using any of these approaches preferrably using data from normal operation.

The papers [4, 14] use the ARX and ARMAX model structure to perform the identification whereas [8] use time domain vector fitting. The papers [4, 8, 14] validated their approaches by comparing the performance of the identified models with measured data. In [9] it was proven, given some technical conditions, that the use of PMU data would indeed result in a consistent estimate of the transfer function used for checking a plant's performance according to the new requirements.

An important contribution from [5], which lays the theoretical foundation for the new draft requirements, is to state stability and performance requirements for hydro power plants in terms of the plants' sensitivity function and disturbance rejection. This a good step towards basing the requirements on well established control system principles. In [11] we used the stability and performance requirements from [5] to show that these requirements can also be checked using PMU measurements. This was demonstrated using measurements from the Norwegian power system. In the current paper we will strengthen the conclusions from [11] by comparing the PMU based approach with the one from [5] using a Monte Carlo Simulation (MCS).

In addition to strengthening the conclusions from [11] the current paper will provide new insight into the identification of hydro power plant dynamics using PMU measurements, with respect to the dataset used, the effect of nonlinearities and the use of power system frequency instead of the electrical angular speed of the machines's rotor.

In [17] it is pointed out that there may be a considerable backlash in the servo of the power plants. Moreover, [3] allows for a deadband on the input to the governor. This means that there are two potential hard nonlinearities that could be detrimental to the identification. In this paper it is checked how large thesse nonlinearities can be before posing a problem, using a MCS approach implemented in Simulink.

An important assumption, when estimating the dynamics of a hydro power plant using PMU measurements, is that the power system frequency close to a generator is a good estimate of the electrical angular speed of its rotor [9]. This assumption is checked in the current paper using a MCS approach and the commercial software PSS/E.

In [6] they describe the identification from the governor input to the electrical power in open loop. This approach is similar to [4, 8] where the transfer function from the electrical frequency to the electrical power is estimated using PMUs. In [14] it was proposed to estimate the transfer function from the power to the frequency. Similarly, [9] also looked at the identification from the electrical power to the frequency. That different papers assume opposite causality may lead to some confusion. In this paper we aim at clearing up this confusion by presenting the relevant transfer functions and discussing the causality. We will also discuss when the different descriptions are valid by considering the fact that the plant can be operated in either closed or open loop during the identification. For the closed loop case we will also investigate what role it plays for the identification whether or not the plant is operated using speed or frequency feedback. To demonstrate the findings from the discussion Monte Carlo Simulations (MCS) are used to compare the results obtained using the different datasets.

The outline of the paper is as follows. In Section 2 the modelling used for a hydro power plant is presented. A brief description of the new draft requirements and our proposal are presented in Section 3.

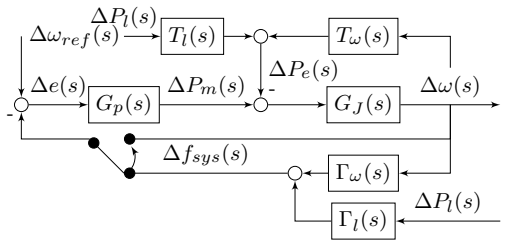

Fig. 1: Block diagram of a hydro power plant

In Section 4 we present the different identification experiments proposed for the identification of hydro power plant dynamics. We also shortly describe the proposed methodology for identifying the plants in Section 5. Results from both simulations and real system data is presented in Section 6 and 7. Finally conclusions and further work are presented in 8.

2 Hydro power plant model

In this section some power system theory needed to understand the rest of the paper is presented. The theory will mostly be presented in the Laplace domain, and we will use s to denote the Laplace operator. To denote a deviation of a variable $x(s)$ around an operating point x_0 we will use the following notation $\Delta x(s) = x(s) - x_0$.

For the power plant model we will assume the structure depicted in Fig. 1. The power plant consists of the transfer functions $G_p(s)$, which represents the governor, servo and turbine dynamics and $G_J(s)$, which represents the swing dynamics of the plant. The swing dynamics relate the electrical angular speed of the machine's rotor $\Delta\omega(s)$ and the electrical and mechanical torque of the machine. This relation is often written using the electrical power $\Delta P_e(s)$ and the mechanical power $\Delta P_m(s)$ of the machine as follows:

$$\Delta\omega(s) = G_J(s)(\Delta P_m(s) - \Delta P_e(s)) \tag{1}$$

From (1) we see that if the electrical power changes the electrical angular speed of the rotor will change. For some of the discussions in this paper the structure of $G_J(s)$ is important. For these discussion we will assume that $G_J(s)$ can be modeled as follows:

$$G_J(s) = \frac{1}{2Hs + K_d} \tag{2}$$

where H is the inertia constant of the machine and K_d is the speed damping.

As already mentioned there will be a change in the electrical angular speed of the rotor when the mechanical power of the turbine does not equal the electrical power of the generator. To contain these changes a frequency containment process (FCP) is implemented which changes the mechanical power of the turbine. It is this process that delivers the FCR. The FCP is represented with the transfer function $G_p(s)$, which acts when the signal $\Delta e(s)$ is nonzero. That is when, the electrical angular speed of the rotor $\Delta\omega(s)$ does not equal its set point value $\Delta\omega_{ref}$. We will not go into further details on the structure of $G_p(s)$ and how the mechanical power $\Delta P_m(s)$ is generated. However, the interested reader may refer to [20].

Often the power system frequency $\Delta f_{sys}(s)$ is used as the feedback signal to the governor instead of the electrical angular speed of the rotor. The reason both the power system frequency and electrical angular speed of the machine's rotor can be used as the feedback signal for the FCP is that the hydro power plants are synchronous generators. This means that we have $2\pi\Delta f_{sys}(j\Omega < \Omega_c) = \Delta\omega(j\Omega < \Omega_c)$ and it is therefore the same to use the power system frequency as the feedback for dynamics slower than Ω_c. Where Ω is the frequency in the frequency domain and Ω_c is the frequency up to which the power system frequency is proportional to the electrical angular speed of the machine's rotor.

For the purpose of identification it is important to analyze how the dynamics of the hydro power plant is excited. From Fig. 1 one can see that it is excited by $\Delta P_e(s)$ and also $\Delta f_{sys}(s)$ if it is operated using the power system frequency as the feedback signal. Fluctuations in these signals are assumed to be due to random load changes $\Delta P_l(s)$, which are assumed to be filtered white noise.

We will start by explaining how the electrical power $\Delta P_e(s)$ is generated. This power is the electrical power at the generator's bus bar, which is approximated by the following expression [2]

$$P_e(t) = \frac{3V_t(t)E_a(t)\sin\delta_{EV}(t)}{X_s} \tag{3}$$

where $V_t(t)$ is the terminal voltage of the machine, $E_a(t)$ is the internal voltage, $\delta_{EV}(t)$ is the angle between the internal voltage and the terminal voltage and X_s is the synchronous reactance. If we linearise (3) assuming the voltages to be constant we get the following equation:

$$\Delta P_e(s) = K_{11}(\Delta\delta(s) - \Delta\delta_V(s)) \tag{4}$$

where K_{11} is a linearization constant $\delta(s)$ is the electrical rotor angle and $\delta_V(s)$ is the voltage angle at the terminal of the generator. We will now rewrite (4) as a function of the random load changes in the system and the angular electrical speed of the machine's rotor.

$$\Delta P_e(s) = T_l(s)\Delta P_l(s) + T_\omega(s)\Delta\omega(s) \tag{5}$$

Where $T_l(s)$ is the transfer function from the random load changes to the voltage angle $\Delta\delta_V(s)$ at the generator terminal and $T_\omega(s)$ is the transfer function from the electrical angular speed of the machine's rotor $\Delta\omega(s)$ to the electrical angle of the rotor $\Delta\delta(s)$ and the voltage angle of the $\Delta\delta_V(s)$ at the generator terminal. In practice the angular speed of the machine's rotor will not greatly influence the voltage angle of the generator terminal and one can therefore normally write $T_\omega(s)$ as:

$$T_\omega(s) = \frac{K_{11}}{s} \tag{6}$$

The power system frequency $\Delta f_{sys}(s)$ is defined as the derivative of the voltage angle $\Delta\delta_V(s)$. It is in general a function of the electrical angular speed of all the synchronous machines in the power system. For our purposes the exact nature of this relation is not important. We will merely assume that the power system frequency can be modeled as follows:

$$\Delta f_{sys}(s) = \Gamma_\omega(s)\Delta\omega(s) + \Gamma_l(s)\Delta P_l(s) \tag{7}$$

where $\Gamma_\omega(s)$ is the transfer function from the electrical angular speed of the machine's rotor to the power system frequency and $\Gamma_l(s)$ is the transfer function from the random load changes to the power system frequency.

3 The new requirements

The theoretical background behind the new requirements is presented in [5]. In short they perform a stability and performance analysis on a model where they have aggregated all power plants together to one plant. They then use a per unit system to formulate the requirement for each plant. The per unit system and aggregated system model used in the draft requirements are presented in the appendix. In [11] we propose to use the same formulation for the stability and performance of the hydro power plant as in [5], however stated for each plant instead of for an aggregated model. The idea is that, although, requiring each hydro power plant to be stable does not guarantee system stability; one unstable plant would give an unstable system. It should therefore as a minimum be required that each plant is stable. Inspired by the idea from [5] the stability margin of the closed loop consisting of the transfer functions $G_p(s)$

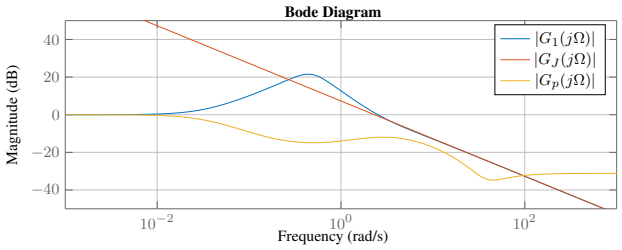

Fig. 2: Comparison of transfer functions

and $G_J(s)$ in Fig. 1 can be estimated using the sensitivity function $S(s)$ as follows:

$$|S(s)| = \frac{1}{|1 + G_p(s)G_J(s)|} < M_s \tag{8}$$

The performance requirement is stated in terms of the system's disturbance rejection. It uses the idea that the power system frequency should fulfill the following constraint $|\Delta f_{sys}(s)| < 0.1Hz$. Since the machines are synchronous we can write this constraint as a constraint on the change in the machine's electrical angular rotor speed due to a change in electrical power as.

$$\Delta\omega(s) = G_J(s)S(s)\Delta P_e(s) = G_1(s)\Delta P_e(s) \tag{9}$$

We now see that if we know the power of $\Delta P_e(s)$ we can put requirements on the plant's disturbance rejection given by $G_1(s)$ to try to keep the frequency deviation below $0.1Hz$.

$$|G_1(j\Omega)| < \frac{\sigma_{\omega_{req}}}{\sqrt{\phi_{P_e}(j\Omega)}} \tag{10}$$

where $\sigma_{\omega_{req}}$ is the variance of the change in electrical rotor speed when it is assumed white and subjected to $|\omega(j\Omega)| < 0.2\pi$ and $\phi_{P_e}(j\Omega)$ is the power of the signal $\Delta P_e(s)$.

In the new draft requirement they propose to find $G_1(s)$ and $S(s)$ by identifying $G_p(s)$ and then to use the estimate together with an estimate of $G_J(s)$, which has been derived from an estimate for the total system inertia of the Nordic Synchronous area. When checking the stability requirements they use an estimate from a low inertia operating state. We will refer to the sensitivity function obtained using the low system inertia as $S_{\min}(s)$. Similarly, they use the average system inertia when finding $G_1(s)$ and we will refer to this estimate as $G_{avg}(s)$.

We will, instead of using a system based estimate for the machine's inertia for the estimate of $G_J(s)$, estimate both $S(s)$ and $G_1(s)$ based on measurements obtained locally at the plant. As was shown in [9] $G_1(s)$ can easily be identified by measuring electrical power and frequency. We will now show how $S(s)$ can be approximated from an estimate of $G_1(s)$ as was shown in [11]. In Fig. 2 we have plotted $G_1(s)$, $G_J(s)$, and $G_p(s)$ for a hydro power plant. The transfer functions are plotted in per unit where the base for $G_p(s)$ is $G_p(0)$ and the base for the two other transfer functions are $G_1(0)$. In the rest of this paper transfer functions will be plotted using this per unit system if not stated otherwise. From the figure one see that the dynamics of $G_1(s)$ are completely determined by the swing dynamics for faster dynamics. Due to the physics of the system this will always be the case. If we now assume the speed damping of the machine to be negligible we can use (2) and interpolation* to obtain the following expression for the machine's inertia

$$H \approx \frac{\Omega_2 - \Omega_1}{2\Omega_1\Omega_2(|G_1(j\Omega_1)| - |G_1(j\Omega_2)|)} \tag{11}$$

We can now find $S(s)$ as follows

$$S(s) \approx 2HsG_1(s) \tag{12}$$

One does not actually need to interpolate, but it is done to average out errors

4 Tests for validating the plants

In the draft requirements [6] they require the power plant owners to estimate the transfer function from the input of the governor to the electrical power at the generator bus bar. Building on this idea, the papers [4] [8] attempts an identification from the power system frequency to electrical power using PMU measurements while the plant is operating in closed loop. However, in [9] we identify the transfer function from the electrical power at the generator bus bar to the machine speed, while the plant is operating in closed loop. To clarify what is the most appropriate approach we will present the transfer functions these different approaches attempt to identify. In addition we will discuss whether or not these transfer functions can be identified for different cases in terms of the available measurements and the feedback signal used for the governor. The cases discussed are as follows:

Case 1: The plant is operating under normal conditions with speed feedback and we have access to the control system signals.
Case 2: The plant is still operating under speed feedback, but we don't have access to the control system signals for the identification and therefore use frequency as an estimate for the speed.
Case 3: The plant is operating with frequency feedback and we have access to the frequency measurements.
Case 4: In this case we have disconnected the input to the governor and replaced it with our own signal, which means the plant is operating in open loop.

4.1 Transfer function from the electrical power to the machine speed $G_1(s)$

We start by looking at the transfer function from the electrical power to the machine speed $G_1(s)$.

$$G_1(s) = -G_J(s)S(s) \tag{13}$$

In [9] **Case 1** was investigated and the result from this investigation is stated in the following proposition.

Proposition 1. *A consistent estimate of $G_1(s)$ can be identified for* **Case 1** *if the following conditions are met:*

Condition C1. *$\Delta P_l(s)$ is persistently exciting.*

Condition C2. *There is a delay in either $G_1(s)$ or $T_\omega(s)$*

Under normal power system operation Condition C1 should hold as there are constant load changes and switching events in the power system. In case Condition C2 does not hold, we may still get a good estimate if the effect of the plant's process noise on the electrical power is small compared to the effect of the random load changes.

For **Case 2** and **Case 3** we will assume the following

Assumption A1. *The measured electrical frequency is a good estimate of rotor speed for slow dynamics if we measure sufficiently close to the generator.*

With Assumption A1 in place we state the following:

Proposition 2. *$G_1(s)$ can be identified for the cases* **Case 2** *and* **Case 3** *if assumption* A1 *holds and conditions* C1 *and* C2 *are met.*

In **Case 4** we are operating in open loop and it will therefore not be possible to identify $G_1(s)$.

4.2 Transfer function from the governor input to the electrical power

According to [6] the power plant owners have to identify the transfer function from the governor's input to the electrical power. This transfer function is given by:

$$G_{req}(s) = \frac{G_p(s)G_J(s)T_\omega(s)}{1 + G_J(s)T_\omega(s)} \tag{14}$$

From (14) we see that the power plant owners will not be required to identify the transfer function used for testing the new requirements. However, it can easily be shown that $G_{req}(\Omega < \Omega_c) \approx G_p(\Omega < \Omega_c)$. We do this by inserting (2) and (6) into (14) to get:

$$G_{req}(s) = \frac{G_p(s)K_{11}}{K_{11} + s(K_d + 2Hs)} \tag{15}$$

From (15) we see that the transfer function one can identify using the measurements as proposed in [6] is the plant transfer function filtered by a second order low pass filter with a resonance frequency of:

$$\Omega_r = \sqrt{\frac{K_{11}}{2H}} \tag{16}$$

Normally, K_d is quite small and one can therefore expect the low pass filter to be underdamped and have a clear resonance peak. Moreover, we will assume $\Omega_c < \Omega_r$.

Since the tests described in [6] are described for open loop operation we will first investigate this case. From [12] we know that an open loop experiment is informative if the input is persistently exciting. From this we have the following proposition.

Proposition 3. *$G_{req}(\Omega < \Omega_c)$ is a good estimate of $G_p(\Omega < \Omega_c)$ and can be identified for* **Case 4** *if the following condition is met*

Condition C3. *$\Delta e(s)$ is persistently exciting*

For the three other cases we can in general not expect to identify $G_{req}(s)$. The reason for this is that the main source of frequency deviations for slow dynamics are due to load changes resulting in the change of generator speeds due to the swing mechanics. In other words, the main excitation to the plant is $\Delta P_e(s)$ not $\Delta f_{sys}(s)$.

Proposition 4. *$G_{req}(s)$ is not possible to identify for* **Case 1**, **Case 2**, *and* **Case 3**.

In summary one should identify the transfer function from the input to the governor and to the electrical power at the generator busbar when performing the identification in open loop and from the electrical power to the electrical angular speed of the rotor or the power system frequency when the plant is operating in closed loop.

5 Methodology

Our proposed methodology for testing whether or not a power plant fulfills the requirements for stability and disturbance rejection uses prediction identification[12]. In this technique we assume that we after the application of an antialiasing filter have collected a data set $Z^N = \{u[n], y[n] | n = 1 \cdots N\}$. The signals in the dataset are assumed generated by

$$\mathcal{S} : y[n] = G_1(z, \theta_0)u[n] + H_1(z, \theta_0)e_1[n] \tag{17}$$

where $G_1(z, \theta_0)$ is the transfer function we want to identify $e_1[n]$ is white noise, $H_1(z, \theta_0)$ is monic, z^{-1} is the time delay operator and θ_0 is the parameter vector parametrizing the true system $\mathcal{S}$. With

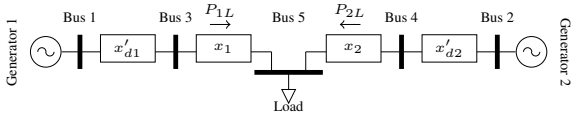

Fig. 3: Small test system

this in place we move on to the aim of prediction error identification, which is to find the parameter vector $\hat{\theta}_N$ such that [12]:

$$\hat{\theta}_N = \arg\min_\theta \frac{1}{N}\sum_{t=1}^{N} \epsilon[n, \theta] \tag{18}$$

with

$$\epsilon[n, \theta] = H_1^{-1}(z, \theta)(y[n] - G_1(z, \theta)u[n]) \tag{19}$$

The identification approach used in the methodology consists of the following steps:

1. The data set Z^N has to be collected while the plant is operating at the desired operating point. Preferably the plant should be operated with speed feedback and the rotor speed should be used as the output signal $y[n]$. If one does not have access to measurements of the rotor speed, a measurement of the frequency can be used instead. For the input signal $u[n]$ one should always use the electrical power of the generator.
2. The next step is to preprocess the data. First one should remove the mean of the collected signals and send them through a low pass filter. For the estimation of the plant's inertia the sample frequency should be chosen such that one can clearly see the slope of the bode plot for the faster dynamics.
3. After the preprocessing the correct model order should be chosen. To do this we suggest to use the box-Jenkins model structure. One easy approach is to start with a high model order and then reduce the model order until one finds the lowest possible model order passing predefined sanity tests for the model.
4. The last step is to estimate the plant's inertia. This can be done by inspecting the slope of the identified bode plot to find where the slope is constant and then apply (11).

6 Simulation results

To test the theory the power system depicted in Fig. 3 was implemented in Simulink. For the modelling of the turbine the non-linear model assuming a non-elastic water column described in [20] was used. For the governor the proportional controller with transient droop described in [20] was used. This combination of turbine and governor is referred to as HYGOV in several simulation softwares. The governor and turbine used the tuning from [16]. Except for the droop at plant 1 which was set to 8% and the droop at plant 2, which was set to 10%. For a complete set of simulation parameters please refer to the appendix. The frequency at the non generator buses were modeled using the frequency divider (FD) equation described in [13].

To excite the system the load was modelled as a wiener process with a standard deviation of $0.4\%[p.u.]$ on system base and a time step of $0.02s$. This choice was made since it resulted in a system where the frequency stayed within the allowed range of $\pm 0.1Hz$. Noise was also added to the generator speed of the two plants. This noise was modelled as white noise processes with standard deviations of $0.004\%[p.u.]$ and $0.04\%[p.u.]$ for plant 1 and 2 respectively. When performing the open loop test for identifying $G_{req}(s)$ white noise with a standard deviation of $0.2\%[p.u.]$ was injected to the governor input. A white noise processes was chosen just for simplicity and other choices are possible. The system base was $30.3GW$ and the machine bases for generator 1 and 2 were $0.3GW$ and $30GW$ respectively. Typically a good sampling rate for dataset when using real data is $2Hz$. However, when obtaining the data sets from

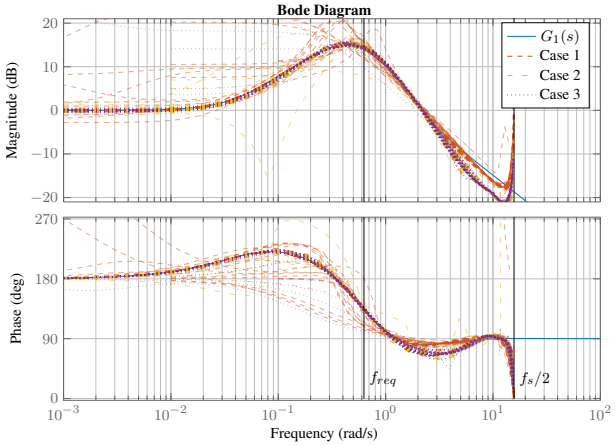

Fig. 4: 100 attempts of identifying $G_1(s)$ for the different cases

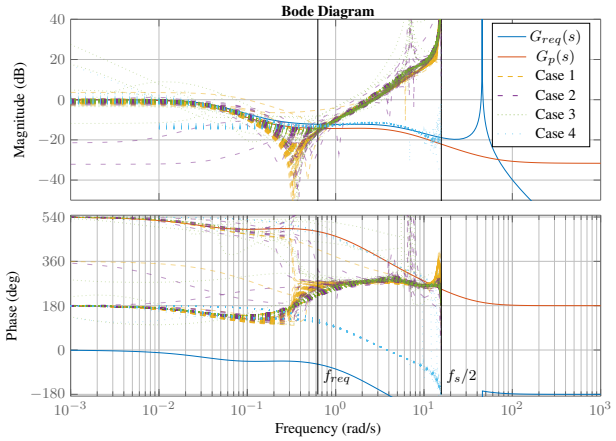

Fig. 5: 100 attempts of identifying $G_{req}(s)$ for the different cases

simulations we sometimes used a sampling rate of $5Hz$ to demonstrate some effects happening at higher frequencies. The sampling rate used can be seen from the figures since the Nyquist frequency is marked in the figures as $f_s/2$.

For all presented simulation results we have performed a simple Monte Carlo Simulation (MCS). That is the Simulink simulations have been run 1000 times with a simulation time of $1800[s]$. For the MCS the effect of the simulation time has not been analyzed. However, in Section 7 it is demonstrated how the accuracy and variability varies with the dataset length. For each run the different noise signals exciting the system have been regenerated to make the run differ from each other. In all the plots we compare all the MCS runs with one analytical representation of the transfer function we are estimating. The analytical transfer function was calculated using the linearization described in [20].

6.1 *Testing of the different cases*

To check the identification of $G_1(s)$ we tested **Case 1**, **Case 2** and **Case 3**. The results from these tests are plotted in Fig. 4, as expected all cases follow the analytical transfer function closely up to a certain frequency. However, one can see that one obtains a small error for the faster dynamics in the cases were we don't have speed feedback and access to the speed measurement. Moreover, **Case 1** and **Case 2** show some more variation for slower dynamics. This may be since **Case 3** has more added excitation. The results are also good for faster dynamics than $f_{req,\max} = 0.1Hz$, which corresponds to the sine wave with the shortest wave length specified in [6].

The results from the identification of $G_{req}(s)$ are provided in Fig. 5. In the figure one can see how the transfer functions $G_p(s)$ and $G_{req}(s)$ follow each other closely until right before the resonance peak, given by (16), as stated in Proposition 3. The identification experiment performed in open loop also follows $G_p(s)$ closely up to the Nyquist frequency, so well beyond what's in the draft requirements. However, it has more trouble converging than the other cases. The convergence trouble could potentially be solved by using a longer dataset or another excitation signal. One should therefore not conclude that this is an inherent problem with this approach before further investigation. For the three other cases one see, as expected, that we don't identify $G_{req}(s)$. It is also interesting to see that the identified transfer function resembles the inverse of $G_1(s)$. Another point worth mentioning is that the result we see in Fig. 5 is the same function presented in the previous papers [4, 8]. These do, however, deviate from $G_p(s)$ before f_{req} and can therefore not be used to check the requirements.

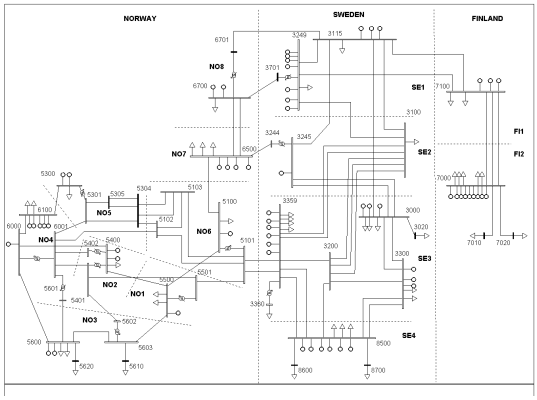

Fig. 6: The Nordic 44 test network from [18]

6.2 *Testing of Assumption* A1 *and effect of nonlinearities*

Since the FD equation provides a rather simplified representation of the power system frequency we also tested **Case 1** and **Case 2** using the commercial power system simulator PSS/E. We used the Nordic 44 power system model depicted in Fig. 6 and described in [19] with the tuning from [16], except for changing the droop of the generator we investigated to 8%. The model was modified by moving one of the plants from its original bus to a new bus connected to the original by a new line modelled as a reactance. This version of the test network can be found in [10]. The identification was performed using the speed of the machine and the frequency of the original bus with an increasing line reactance.The simulation was run 100 times with a simulation time of $1200[s]$. A shorter simulation time was chosen for the PSS/E simulations than for the MATLAB simulations as we experienced problems with the software when running for $1800[s]$. The result of this is plotted in Fig. 7, where one can see that using the frequency instead of the speed gives an incorrect estimate of the swing dynamics. This corresponds with the findings in Fig. 4.

The effect of different deadbands are presented in Fig. 8. In [3] the maximum allowed deadband for certain power plants are given to be $0.5Hz$, which corresponds to $1\%p.u.$. From the figure one can see that with this value no identification is possible as long as the frequency stays within its allowed range. With a value of $0.05\%p.u.$ the results are quite good. For all other cases the results are not really reliable. However, with a deadband of $0.1\%p.u.$ one should be careful as the shape of the plot still remains reasonable.

How the backlash affects the results are presented in Fig. 9. For the test of the backlash we start with a value at one tenth of what is

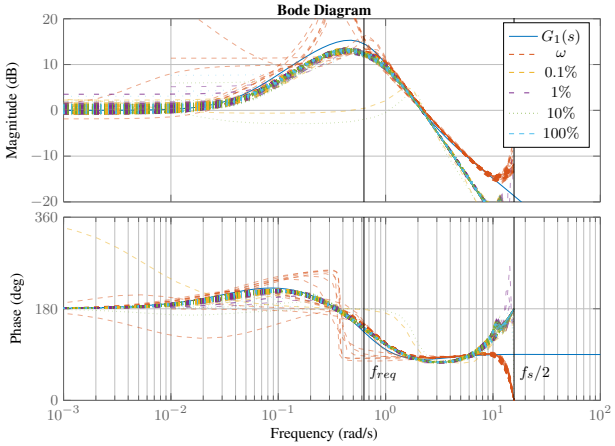

Fig. 7: Identification with different reactances

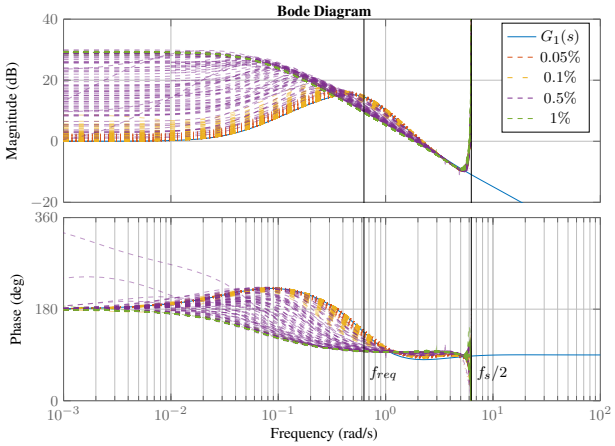

Fig. 8: Testing different deadbands

reported in [17], which doesn't give any problems. The next value corresponds to the value reported in [17] and with this value one can see that the identification is incorrect for higher frequency dynamics. When the backlash is further increased by a factor of 10 the results are not anywhere near correct.

6.3 Comparison of our approach and the one in the draft requirements

To compare our proposal for testing the requirements with the one proposed in [5] we have in Fig. 10 plotted the amplitude of the sensitivity function calculated, analytically, with our approach denoted $|S(e^{j\Omega}, \hat{\theta})|$, and the approach from [5] denoted $|S_{\min}(e^{j\Omega}, \hat{\theta})|$. From the figure one can see that $S(z, \hat{\theta})$ is a better estimate than $S_{\min}(z, \hat{\theta})$ around the peak of the sensitivity function, which is the value we want to check. The peak value of the sensitivity functions are reported in TABLE 1. From the table one can see that the method proposed in the draft requirements overestimates the stability margin. The approaches where one does not have the speed measurements on the other hand underestimates the stability margin. A comparison of the estimated inertia constants for the three first cases are presented in TABLE 2. As one would expect **Case 1** is clearly the best.

The function $G_1(s)$ is also plotted together with two estimates in Fig. 11. In this case the estimate obtained using $G_{J_{\min}}(s)$ clearly shows a better performance in terms of disturbance rejection than what's actually the case.

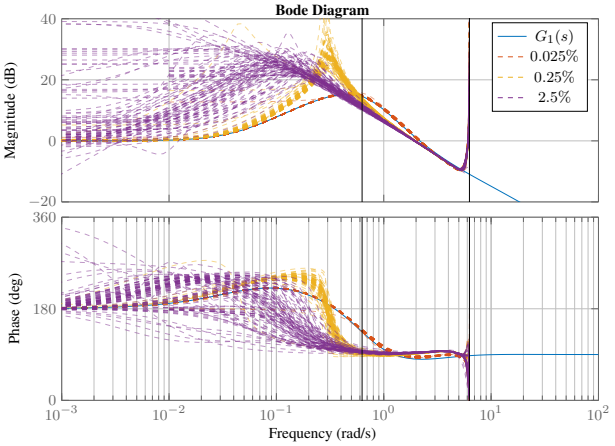

Fig. 9: Testing different backlasch

Table 1 Maximum values of sensitivity functions

Method	Median	Root mean square error (RMSE)
$\max \lvert S(j\Omega)\rvert$	1.84	0
$\max \lvert S(e^{j\Omega}, \hat{\theta})\rvert$, **Case 1**	1.84	0.25
$\max \lvert S(e^{j\Omega}, \hat{\theta})\rvert$, **Case 2**	1.75	0.34
$\max \lvert S(e^{j\Omega}, \hat{\theta})\rvert$, **Case 3**	1.74	0.39
$\max \lvert S_{\min}(e^{j\Omega}, \hat{\theta})\rvert$	1.66	0.25

Table 2 Estimated inertias

Case	Median	RMSE
Actual	3.5	0
Case 1	3.40	0.46
Case 2	3.33	0.40
Case 3	3.27	0.43

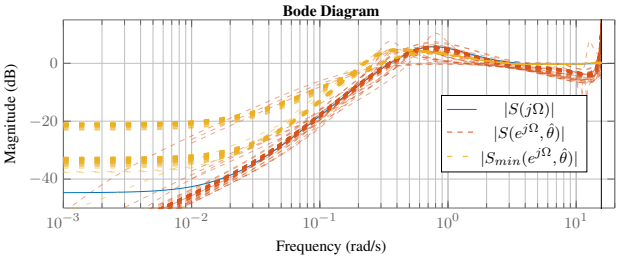

Fig. 10: The sensitivity function calculated using our approach and the one from [5]

7 Results from power plants in the Norwegian system

7.1 Comparison of PMU approach and draft requirements

To test the methodology on real data we will use data from a test run by Statkraft on one of their power plants and PMU measurements from the same plant. The turbines in the plant are Pelton turbines. This is an advantage as the servos for such turbines are not expected to have any considerable backlash. The one line diagram of the relevant part of the plant is shown in Fig. 12. The PMU data was collected from the high voltage side of the step up transformer in February 2016, while the plant was in normal operation. Since the generators are very close to each other we assume they can be treated as one. The signals collected using the PMU and the ones provided

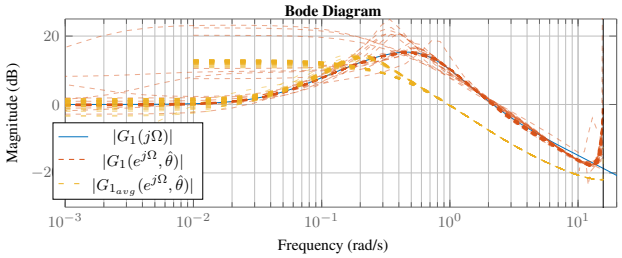

Fig. 11: The disturbance rejection function calculated using our approach and the one from [5]

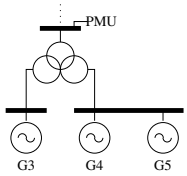

Fig. 12: One line diagram of the plant

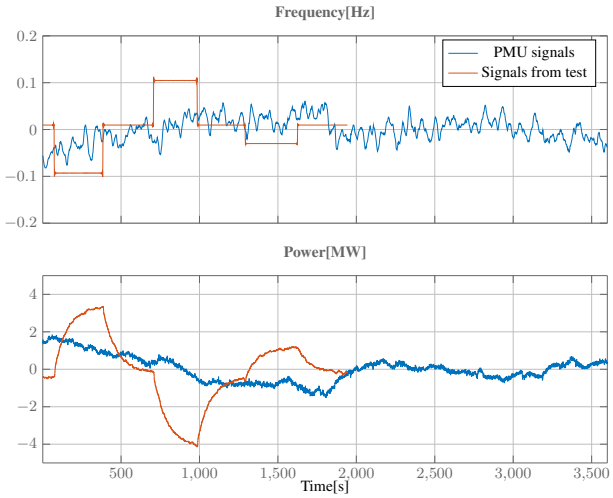

Fig. 13: Dataset collected using PMU and test at the plant

by Statkraft after it has been filtered and detrended are presented in Fig. 13.

The bode plot of the identified plant using PMU data is presented in Fig. 14, together with its 95% confidence interval. From the plot one can see that it resembles that of $G_1(s)$ presented from the simulations, and that it has low variance. In this case the bode plot is not plotted using per unit.

To check the identification of the transfer function $G_{req}(s)$ we will use data from a test performed by Statkraft at the same plant. During the test all the generators at the plant were operated with speed feedback except $G4$, and $G5$, which were fed a signal from a signal generator. During the tests both sinusoids and step signals were injected to the governor. Since a step contains all frequencies we will use one of the step tests for the identification.

In Fig. 15 attempts of identifying $G_{req}(s)$ during both open and closed loop operation are presented. The data for the closed loop operation comes from the PMU and the data for open loop operation comes from the step test. One can observe that the result obtained for the closed loop operation resembles that of Fig. 5, which further supports the statement that the plant should be operated in open loop to be able to identify $G_{req}(s)$. The results obtained from the open loop

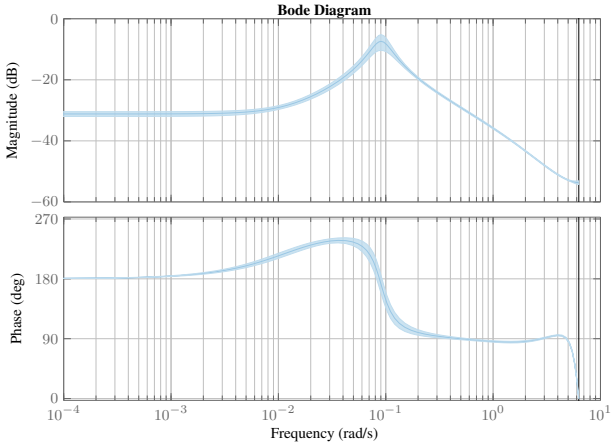

Fig. 14: $G_1(s)$ identified using PMU measurements

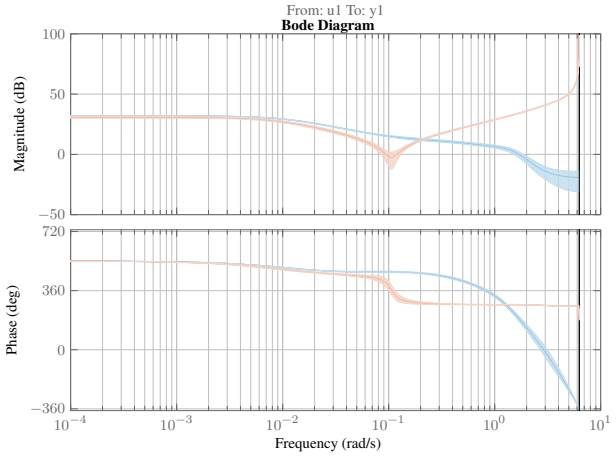

Fig. 15: Attempts of identifying $G_{req}(s)$ in closed and open loop operation

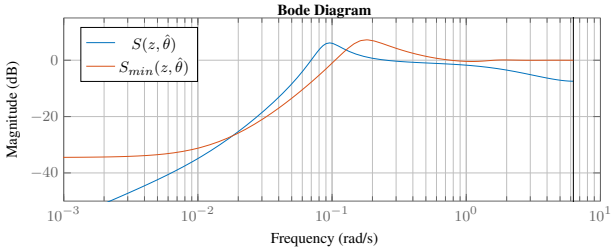

Fig. 16: The sensitivity function calculated using our approach and the approach from [5]

operation on the other hand looks reasonable, however, the variance is increasing significantly for the faster dynamics. As in the previous plot this plot is not in per unit.

We also compared the estimate for the sensitivity function and $G_1(s)$ in Fig. 16 and Fig. 17. In this case both estimates are much closer to each other than the case was for the simulations. This is obviously something that can happen since some plants may have similar swing dynamics as the average system. The main point, however, remains that one may as well check the requirements using PMU measurements instead of using the approach proposed in [6].

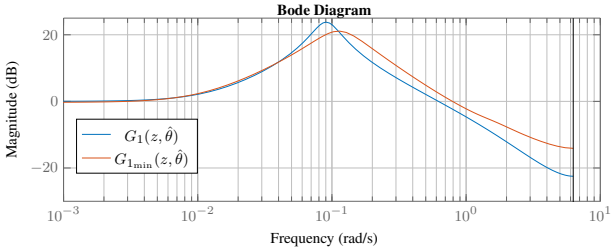

Fig. 17: The sensitivity function calculated using our approach and the one from [5]

Table 3 Droop setting and $G_1(0)$

Droop	$60min$	$45min$	$30min$	$15min$
10%	9.5%	9.5%	9.5%	9.5%
6%	6.2%	6.0%	5.9%	6.1%
5%	4.9%	4.9%	5.0%	5.1%
3%	3.1%	3.1%	3.1%	2.9%
2%	2.0%	1.8%	1.8%	1.7%

7.2 Results from a plant operating in closed loop and using control system measurements instead of PMU

When using PMU measurements for obtaining the estimate one have to keep in mind that there may be some losses in the active power of the plant, which are not accounted for. In addition the closer to the generator one measures the power system frequency the better we can assume it to estimate the electrical angular speed of the machine's rotor. It is therefore of interest to see how our approach performs when one uses measurements obtained as close as possible to the generator. This can be achieved if one has access to the control signals of a modern hydro turbine governor. This is for our purpose the same as placing a PMU on the generator terminal.

Another advantage of having access to the control system is that it allows us to test if the method is able to capture changes in the governor parameters. We therefore did a test at one of Statkraft's power plants where we connected a computer to the control system of the governor. The tests consisted of letting the plant run for one hour, before we changed the governor parameters. The plant was also set to operate with a constant load during the tests. While the parameters where changed we did not record anything, which means that the datasets may be a few minutes shorter than one hour. An example of a dataset is presented in Fig. 18. This dataset was obtained with a droop setting of 2%.

Based on the tests performed on the other power plant, new parameters for the PID part of the governor was calculated. Although, these parameters were calculated for another plant we compared these new parameters with the old parameters for this plant. A result of this is shown in Fig. 19, where one can see that the proposed approach can indeed detect the parameter change. One can also see that the new parameters give a better disturbance rejection than the old parameters.

We also tested several different droop settings. The result of this is given in Fig. 20. All the estimates in this figure is performed while the plant is operated using the new PID parameters. However, for the droop setting of 10% and 6% a smaller proportional gain is used than for the other cases. One can clearly see that the approach captures both the change in the droop and the proportional gain. The approach's sensitivity to different lengths of the dataset is demonstrated in Fig. 21, where one can see that the results are quite reasonable for all lengths except for the 15 minutes dataset. The steady state gain for the transfer functions in Fig. 20 is presented together with the droop setting in Table 3 for different lengths of the datasets. As expected the values are quite close.

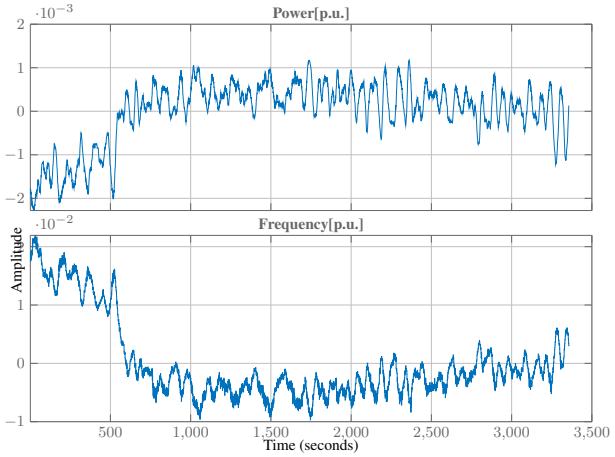

Fig. 18: Signals from control system

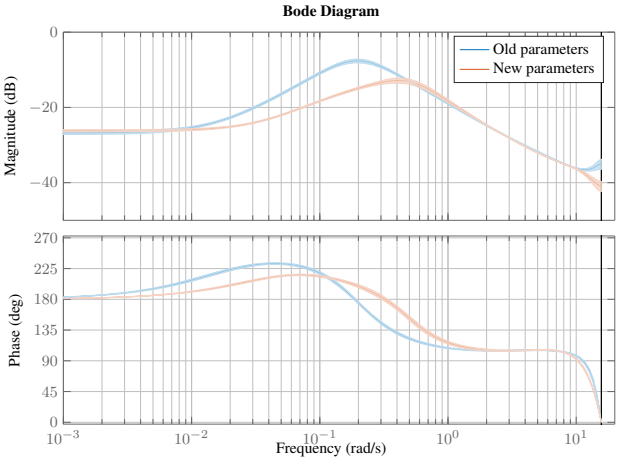

Fig. 19: Estimate of $G_1(s)$ new and old tuning

8 Conclusions and further work

In this paper we have presented a method for testing a hydro power plant's stability margin and disturbance rejection using PMU and control system measurements. The main advantage of the proposed method is that it is almost non-intrusive. That is the tests can be performed while the power plant is in normal operation, with the only restrictions that the scheduled power production of the plant should remain constant during the test. Furthermore, the best results are obtained if one has access to measurements of the rotor's speed, since this allows for obtaining a good estimate of the plant's inertia. Otherwise, one can use measurements of frequency and one should get an estimate which is not any worse than what one would get using the method proposed in the recent draft requirements for FCR providers in the Nordic synchronous area.

The estimate of the stability margin and distrubance rejection obtained using the proposed method is also closer to the analytical calculated values than what one obtain using the method proposed in the draft requirements. However, the method is most applicable to power plants where there is no have a significant input deadband or backlash. Input deadband is sometimes set intentionally to prevent wear and tear of the power plant components and may in some cases be avoided. Backlash, on the other hand mostly depends on the type of turbine. Generally, one can expect a significant backlash in Kaplan turbines and high pressure Francis turbines. For these types of turbines the method proposed in the draft requirements could be used as it handles backlash better.

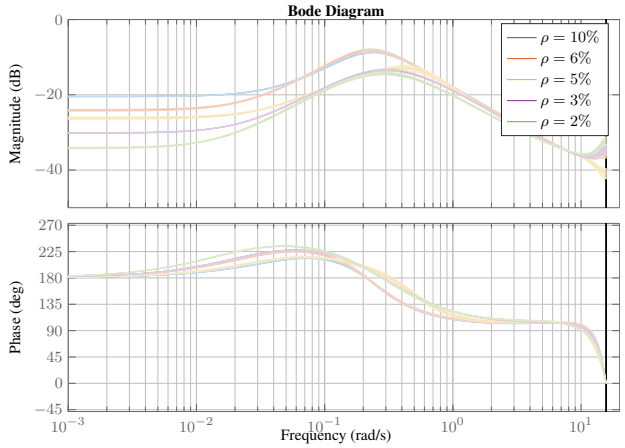

Fig. 20: $G_1(s)$ with different droop settings

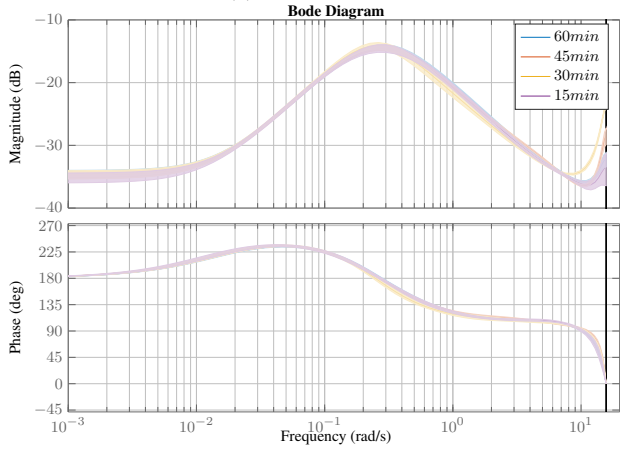

Fig. 21: $G_1(s)$ obtained using different signal length

It should be noted that if one uses PMU measurements for the identification, the faster dynamics will be estimated incorrectly. This is due to the rotor angle dynamics of the generator and the fact that the electrical frequency is only a good estimate of the angular speed of the machine's rotor for slower dynamics. This effect is demonstrated in the simulation study. However, the obtained estimates are still satisfactory when we are mostly interested in the turbine and governor dynamics.

We also discussed the different input output combinations that have been attempted in the literature for identification of hydro power plant dynamics using PMUs. Here we argued that one should use the electrical power as the input signal and the power system frequency as the output signal. This was also demonstrated through simulations.

In summary, the proposed method can serve as either an alternative or a supplement to what is proposed in the draft requirements. A potential advantage with our method is that it allows for online implementation since the identification can be done while the plant is in normal operation.

9 References

1 H.G. Aghamolki, Z. Miao, L. Fan, W. Jiang, and D. Manjure. Identification of synchronous generator model with frequency control using unscented Kalman filter. *Electric Power Systems Research*, 126:45–55, 2015.

2 Stephen J. Chapman. *Electric machinery and power system fundamentals*, volume 3. McGraw-Hill New York, 2002.

3 European Commission. Network Code on Requirements for Grid Connection Applicable to all Generators, April 2016.

4 Dinh Thuc Duong, Kjetil Uhlen, Stig Løvlund, and Erik Alexander Jansson. Estimation of Hydro Turbine-Governors Transfer Function from PMU Measurements. Boston, July 2016. IEEE.

5 Robert Eriksson, Niklas Modig, and Andreas Westberg. FCR-N DESIGN OF REQUIREMENTS. ENTSO-E report, July 2017.

6 Prequalification Working Group. Technical Requirements for Frequency Containment Reserve Provision in the Nordic Synchronous Area. Draft, June 2017.

7 N. D. Hatziargyriou, E. S. Karapidakis, G. S. Stavrakakis, I. F. Dimopoulos, and K. Kalaitzakis. Identification of synchronous machine parameters using constrained optimization. In *Power Tech Proceedings, 2001 IEEE Porto*, volume 4, pages 5 pp. vol.4–, 2001.

8 S. H. Jakobsen and K. Uhlen. Vector fitting for estimation of turbine governing system parameters. In *2017 IEEE Manchester PowerTech*, pages 1–6, June 2017.

9 S. H. Jakobsen, K. Uhlen, and X. Bombois. Identification of hydro turbine governors using PMU data. In *2018 IEEE International Conference on Probabilistic Methods Applied to Power Systems (PMAPS)*, pages 1–6, June 2018.

10 Sigurd Hofsmo Jakobsen. N44 test network. 2018.

11 Sigurd Hofsmo Jakobsen, Kjetil Uhlen, and Petter Lie. System identification techniques for validating hydro power plants FCR performance. Aalborg, June 2019. Cigre.

12 Lennart Ljung. *System identification*. Springer, 1998.

13 F. Milano and Á Ortega. Frequency Divider. *IEEE Transactions on Power Systems*, 32(2):1493–1501, March 2017.

14 B. Mogharbel, L. Fan, and Z. Miao. Least squares estimation-based synchronous generator parameter estimation using PMU data. In *2015 IEEE Power Energy Society General Meeting*, pages 1–5, July 2015.

15 J. C. N. Pantoja, A. Olarte, and H. Díaz. Simultaneous estimation of exciter, governor and synchronous generator parameters using phasor measurements. In *2014 Electric Power Quality and Supply Reliability Conference (PQ)*, pages 43–49, June 2014.

16 T. J. M. A. Parreiras, S. Gomes, G. N. Taranto, and K. Uhlen. Closest security boundary for improving oscillation damping through generation redispatch using eigenvalue sensitivities. *Electric Power Systems Research*, 160:119–127, July 2018.

17 L. Saarinen, P. Norrlund, and U. Lundin. Field Measurements and System Identification of Three Frequency Controlling Hydropower Plants. *IEEE Transactions on Energy Conversion*, 30(3):1061–1068, September 2015.

18 Silje Mork Hamre. Inertia and FCR in the Present and Future Nordic Power System. Master's thesis, Norwegian University of Science and Technology, Trondheim, June 2015.

19 Luigi Vanfretti, Svein H. Olsen, V. S. Narasimham Arava, Giuseppe Laera, Ali Bidadfar, Tin Rabuzin, Sigurd H. Jakobsen, Jan Lavenius, Maxime Baudette, and Francisco J. Gómez-López. An open data repository and a data processing software toolset of an equivalent Nordic grid model matched to historical electricity market data. *Data in Brief*, 11:349–357, April 2017.

20 Working Group on Prime Mover and Energy Supply Models for System Dynamic Performance Studies. Hydraulic turbine and turbine control models for system dynamic studies. *IEEE Transactions on Power Systems*, 7(1):167–179, February 1992.

Appendix

per unit system used in the requirements

In the draft requirements they assume the system model depicted in Fig. 22, where $G_{p_{sys}}(s)$ is the aggregated response of all the turbines, servos and governors in the system and $G_{J_{sys}}(s)$ is the aggregated swing dynamics of the system. The transfer function $D(s)$ represents the transfer function from the aggregated load to the aggregated swing dynamics. The stability requirements are then expressed in terms of the norm of the sensitivity function of the aggregated system.

$$|S_{sys}(s)| < M_s \tag{20}$$

where

$$S_{sys}(s) = \frac{1}{1 + G_{J_{sys}}(s)G_{p_{sys}}(s)} \tag{21}$$

and M_s is a constant.

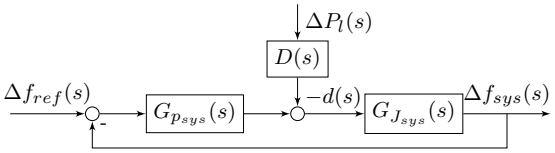

Fig. 22: Model used in [5]

The performance requirement is stated in terms of the system's disturbance rejection. It uses the idea that the power system frequency should fulfill the following constraint $|\Delta f_{sys}(s)| < 0.1Hz$. The change in the power system frequency is given by the following equation

$$\Delta f_{sys}(s) = -2\pi G_{J_{sys}}(s) S_{sys}(s) d(s) = G_{1_{sys}}(s) d(s) \quad (22)$$

We can now write the power spectral relation between the random load changes and the change in power system frequency as:

$$|S_{sys}(j\Omega)|^2 \phi_{P_l}(j\Omega) = \frac{1}{2\pi |D(j\Omega) G_{J_{sys}}(j\omega)|^2} \phi_f(j\Omega) \quad (23)$$

where $\phi_{P_l}(j\Omega)$ is white noise with power spectral density (PSD) equal to one and $\phi_f(j\Omega)$ is the psd of the power system frequency with the value σ_f^2. The performance requirement is thus stated as:

$$|S_{sys}| < \frac{\sigma_f}{|D(s) G_{J_{sys}}(s)|} \quad (24)$$

To test whether or not the plants fulfill the requirements [5] suggests that the power plants owners estimate the transfer function $G_p^{(p.u.)}(s)$ for their plant. This function is to be multiplied with $G_{J_{sys}}^{(p.u.)}(s)$ to check the requirements. To explain the rational behind this we start by defining the per unit base for a plant as it's static gain

$$G_p^{base} = G_p(0) \quad (25)$$

For the system base we will use the sum of all the static gains of the plants in the system, that is

$$G_{J_{sys}}^{base} = \frac{1}{\sum_i^{N_g} G_{p_i}(0)} \quad (26)$$

If we now look at the sensitivity for the whole system we get.

$$S_{sys}(s) = G_{J_{sys}}(s) G_{p_{sys}}(s) = G_{J_{sys}}(s) \sum_i^{N_g} G_{p_i}(s)$$

$$G_{J_{sys}}(s) \sum_i^{N_g} G_{p_i}(s) \frac{G_{p_i}(0)}{G_{p_i}(0)} \approx G_{J_{sys}}^{(p.u.)}(s) G_p^{(p.u.)}(s) \quad (27)$$

In the last step of (27) we have assumed all plants $G_{p_i}(s)$ to be approximately equal to each other. We will now introduce two different versions of $G_{sys}(p.u.)$. Namely, $G_{J_{\min}}^{(p.u.)}$ and $G_{J_{avg}}^{(p.u.)}$ these are the system transfer functions for the system with the minimum amount of inertia and with the average amount of inertia. From now on we will assume everything to be in per unit if not stated otherwise. The requirement for stability and performance are thus stated as follows

$$|S_{\min}(s)| = \frac{1}{|1 + G_p(s) G_{J_{\min}}|} < M_s \quad (28)$$

$$|S_{avg}| < \frac{\sigma_f}{|D(s) G_{J_{avg}}(s)|} \quad (29)$$

Where $G_{\min}(s)$ and $G_{avg}(s)$ are assumed to be given by

$$G_{sys}(s) = \frac{600MW}{0.1Hz} \frac{f_0}{S_{sys}} \frac{1}{2H_{sys}s + K_{d_{sys}} f_0} \quad (30)$$

Simulation parameters

Table 4 The parameters used for Fig. 3

Variable	Explanation	Value	
S_1	Machine 1 base power	$300MW$	-
S_2	Machine 2 base power	$3GW$	-
S_{base}	System base power	$3.3GW$	-
U_{base}	Base voltage for the transmission system	$400kV$	-
U_M	base voltage for the machines	$20kV$	-
D	Proportional load frequency dependency	50	S_{base}
H_1	Generator 1 inertia constant	3.5	
H_2	Generator 2 inertia constant	$9.68s$	
K_{d1}	Damping constant	0.1	-
k_{d2}	Damping constant	0.1	-
x_1	Reactance between bus 3 and 5	0.5	S_{base}
x_2	Reactance between bus 4 and 5	0.5	S_{base}
x_{d1}	Sub transient reactance generator 1	0.15	S_1
x_{d2}	Sub transient reactance generator 2	0.15	S_1

Table 5 Hydro turbine governor parameters

Variable	Explanation	Value
T_f	Low pass filter time constant	$0.2s$
T_r	Droop time constant	$5s$
r	Temporary droop	0.3
ρ_1	Droop	0.08
ρ_2	Droop	0.1
T_y	Servo time constant	$0.2s$
T_w	Water starting time	$1.01s$
q_{nl}	No load flow	0.1
h_s Static head of water column	1	
A_t Turbine gain	1	